UNCLASSIFIED

AD 255 718

Reproduced
by the

ARMED SERVICES TECHNICAL INFORMATION AGENCY
ARLINGTON HALL STATION
ARLINGTON 12, VIRGINIA

UNCLASSIFIED

NOTICE: When government or other drawings, specifications or other data are used for any purpose other than in connection with a definitely related government procurement operation, the U. S. Government thereby incurs no responsibility, nor any obligation whatsoever; and the fact that the Government may have formulated, furnished, or in any way supplied the said drawings, specifications, or other data is not to be regarded by implication or otherwise as in any manner licensing the holder or any other person or corporation, or conveying any rights or permission to manufacture, use or sell any patented invention that may in any way be related thereto.

NASA TN D-868

CATALOGED BY ASTIA
AS AD No. 257714

NOX

TECHNICAL NOTE
D-868

EXPERIMENTAL INVESTIGATION OF STAGE SEPARATION AERODYNAMICS

By Robert A. Wasko

Lewis Research Center
Cleveland, Ohio

ASTIA
MAY 11 1961
TIPDR B

NATIONAL AERONAUTICS AND SPACE ADMINISTRATION
WASHINGTON

602100

May 1961

N

NATIONAL AERONAUTICS AND SPACE ADMINISTRATION

TECHNICAL NOTE D-868

EXPERIMENTAL INVESTIGATION OF STAGE SEPARATION AERODYNAMICS

By Robert A. Wasko

SUMMARY

Interstage aerodynamic pressure that occurs during stage separation was investigated for a two-stage missile at a Mach number of 2.0 and an altitude of 38,000 feet in the NASA Lewis 8- by 6-foot supersonic wind tunnel. The model consisted of a wing-supported second stage having a cold-air simulated rocket motor operated at a constant total pressure, and a sting-supported, translating first stage. Separation distance was varied up to 3 second-stage body diameters. Effects of stage misalinement were studied by displacement of stage centerlines over a range up to 1 second-stage diameter. First- to second-stage diameter ratios were 1.0, 1.25, and 1.5.

First-stage interference effects produced higher-than-ambient second-stage base pressures over a longer separation distance for jet-off staging than for jet-on. First-stage ports for rocket-on staging reduced the distance of first-stage interference effects. Ports also reduced but did not eliminate fluctuating second-stage base and afterbody pressures that occurred at separation distances less than 1 diameter for rocket-on staging.

INTRODUCTION

Successful use of stage separation techniques for both jet-off and jet-on staging depends on an understanding of the pressures and forces experienced by separating stages, particularly in the interstage area. The mutual aerodynamic interactions that occur between the stages during separation are not readily amenable to calculation, particularly for jet-on staging where the upper-stage rocket motor is operating while the stages are still attached. Further, very little experimental data on the fundamental aspects of the problem exist.

This report therefore presents the results of a preliminary experimental investigation into the aerodynamics of rocket-on and rocket-off stage separation. A model of a two-stage missile having a cold-flow second-stage rocket motor was tested in the 8- by 6-foot supersonic wind

tunnel at a free-stream Mach number of 2.0 at a pressure altitude of 38,000 feet. It was intended that this investigation would demonstrate heretofore undescribed aerodynamic phenomena that occur during stage separation, thus providing a foundation for subsequent investigations. In addition, the advent of multistaged vehicles with mega-pound-thrust boosters and high-energy upper stages (such as the advanced Saturn configurations), as well as interest in short-range two-stage missiles, indicates the possibility of stage separation at Mach numbers and altitudes near those of the test conditions.

SYMBOLS

D body diameter

L distance between separating stages

l distance downstream of first-stage forebody leading edge

M Mach number

P total pressure

p static pressure

x distance upstream of second-stage base

Y displacement of first- and second-stage body centerlines

Subscripts:

a afterbody

b base

j jet

0 free-stream conditions

1 first stage

2 second stage

APPARATUS AND PROCEDURE

The model of the two-stage missile is shown schematically in figure 1(a). The second stage was a wing-mounted, closed-base model 73.5 inches long, having an 8-inch-diameter cylindrical body with a 20° conical nose.

The first stage consisted of a sting-mounted hydraulically movable cylinder approximately 42 inches long. Three first stages were used, having body diameters of 8, 10, and 12 inches, resulting in first- to second-stage diameter ratios of 1.0, 1.25, and 1.5, respectively. The forebodies of the 10- and 12-inch models were truncated cones with 10° half-angles.

The second-stage jet was simulated with cold air exhausting through a convergent-divergent nozzle of area ratio 2 (fig. 1(b)) at a jet total-pressure ratio $P_j/p_0 = 40$. This area ratio was arbitrarily picked as that which would give a large jet-exit to free-stream static-pressure ratio for a limiting supply pressure of 125 pounds per square inch absolute. Jet-exit to afterbody diameter ratio D_j/D_a was 0.325.

First-stage port designs, shown in figure 2, were arbitrarily based on determining the area necessary to pass the entire jet exhaust assuming choking at a total pressure equal to jet-exit static pressure. The area was then divided into four slots of equal area, symmetrically distributed about the forebody circumference. Cones located within the first-stage cavity were used as flow deflectors (fig. 2). These deflectors were designed so that the base of the cone would coincide with the shoulder of the forebody and that the cone angle would be sufficient to allow accommodation of a hypothetical hemispherical-topped propellant tank inside the first stage.

Instrumentation details are shown in figure 3. The second stage (fig. 3(a)) was instrumented with static-pressure orifices on the base and on the top and bottom of the afterbody in a plane normal to the plane of the strut. Since pressure instrumentation was in this plane, strut wake effects on the measured pressures were considered negligible. A pressure transducer in the base was used to ascertain unsteady base pressures.

The first stage (fig. 3(b)) was instrumented with static-pressure orifices on the top and bottom external surfaces of the forebody and for the unported configuration on the bulkhead inside the forebody cavity. For the ported configurations, the flow deflectors excluded the bulkhead statics.

The test was conducted at a free-stream Mach number 2.0 and a pressure altitude of approximately 38,000 feet. Stage separation was accomplished by translating the piston-mounted first stage $3\frac{1}{2}$ inches for each of two longitudinal positions of the sting mount, thereby giving a separation range from 0.1 to 22 inches (0.0125 to 2.8 second-stage diameters). With the strut in its most forward position, the first stage was translated downstream over the range of separation distances from 0.0125 to 1.07 diameters while the jet was continuously in operation.

The tunnel operation was then interrupted and the strut moved 14 inches downstream. After tunnel operations had resumed, the rocket was again operated at constant flow while translating the first stage aft over the range of separation distances from 1.77 to 2.8 diameters. Data curves were extrapolated between separation distances of 1.07 and 1.77 diameters.

RESULTS AND DISCUSSION

Jet-Off

Figure 4 shows the first-stage external pressure distribution for jet-off at several separation distances. Pressures along the top and bottom surfaces were essentially equal. For the configurations with $D_1/D_2 = 1.5$ and 1.25, the sharp decrease in pressure ratio due to expansion about the forebody shoulder can be noted. At initial separation distances, pressures prior to the expansion were between that corresponding to a 10°-conical and a 10° two-dimensional deflection at a Mach number of 2.0. As separation distance increased, these pressures approached that for a 10°-conical deflection. As expected, the pressures for the $D_1/D_2 = 1.0$ configuration were essentially constant and approximated free-stream static pressure.

Variations of second-stage base pressure and first-stage forebody and internal pressures with separation distance are shown in figure 5. Forebody pressures are those measured near the leading edge. Internal pressures are those measured on the bulkhead and are representative of relatively constant pressures within the cavity. For all diameter ratios, internal pressures were equal to second-stage base pressures for separation distances up to about 0.2 diameter, but at greater distances they increased with separation distances since more of the cavity was exposed to the free stream. First-stage interference effects kept the base pressures greater than p_0 for separation distances up to about 2.8 diameters. Increasing stage diameter ratio increased base pressure ratio for separation distances up to 1.8 diameters; but at greater distances, diameter ratio had little effect.

Interstage flow during stage separation is similar to that of axisymmetric rearward-facing steps, which are discussed in reference 1. Using this analogy, it can be seen that second-stage base pressures are strongly dependent on the shock system of the first-stage forebody. However, analysis of interstage base flow is more complicated than that of the simple step configurations because, unlike the later, the trailing shock originated near the forebody leading edge. Thus, the leading edge can increase the trailing-shock pressure rise.

E-1102

Lateral displacement of stage centerlines, such as may occur because of stage misalinement during separation, caused unstable interstage flow similar to inlet buzz. Figure 6 shows the lateral displacement at which buzz occurs. The boundary between buzz and no-buzz regions was not always precisely defined for any configuration; therefore, the shaded area indicates general limits determined with all three diameter ratios. The possibility of the first stage striking the motor precluded obtaining data for separation distances less than 0.37 diameter. Sensitivity to buzz for lateral displacement of centerlines decreased with increasing separation distance.

Jet-On

Figures 7 and 8 show first-stage external pressure distributions at several separation distances for the nonported and ported configurations, respectively. For the nonported configurations, pressures near the forebody leading edge were lower than the jet-off pressures as a result of expansion of the jet flow over the forebody leading edge. The effect of ports was to decrease the amount of jet flow being spilled around the forebody leading edge, thereby increasing pressures in this region to values approaching jet-off surface pressures. At stations farther downstream from the leading edge, local irregularities in pressure distributions were present as a result of free-stream and ported-flow interaction.

Figures 9 and 10 show pressure distributions along the internal surface of the first-stage forebody for the nonported and ported configurations, respectively. Pressures for the nonported configuration were somewhat less near the leading edge than they were deeper in the cavity, and the general level increased gradually with separation distance. For the ported configurations the pressures near the leading edge were about the same as with the unported configurations, but at distances deeper into the cavity there were sharp variations that were probably associated with an internal-shock structure of the ported flow.

The effect of the rocket exhaust on base pressures is shown in figure 11, and jet-off data are repeated from figure 5 for comparison. Because of unsteady base flow, jet-on data were not obtained for separation distances less than 0.37 diameter for the ported configurations and 1.07 diameters for the nonported configurations. At small separation distances, base pressures for both the ported and nonported configurations were much higher than jet-off base pressures. However, as separation distance increased, the interference effects diminished more rapidly than with the jet-off; the base pressure ratio approached a constant value of about 0.4. In one case ($D_1/D_2 = 1.5$, ports) the sharp drop in base pressure occurred in the range of separation distances where jet operation was interrupted to reposition the first-stage strut, and hence details of this pressure decrease were not determined.

The base flow resulting from the simple interaction of a jet and the stream without interference effects of a first stage has been described in reference 2. As discussed there, base pressure is dependent upon the trailing-shock pressure rise that occurs at the intersection of the jet and stream. In the present test, interference effects of the first stage on base flow would be expected to occur when the shape of the jet in the region of the jet-stream intersection is modified by the presence of the bow wave in front of the blunt first stage, thereby modifying the strength of the trailing-shock pressure rise. The result was increased base pressures.

For all configurations, the use of ports caused the interference effects to diminish at smaller separation distances than with the nonported configurations. This trend was expected for two reasons. First, the use of ports would decrease the distance that the bow wave would extend upstream of the first stage and hence reduce the extent of base flow interaction. Second, the use of ports diminished the quantity of reversed flow, which at small separation distances entered directly into the base region without first undergoing jet-stream interaction; hence, base pressures at a given separation were lowered and interstage flow was stabilized.

With the ports, the base flow may be even further modified by an effect of the interaction of the stream with the jet flow issuing from each of the ports. The magnitude of this effect would depend upon, among other things, the location of the ports downstream of the forebody leading edge. With these particular models, as shown in figure 2, this distance increased with increasing diameter ratio.

The high base pressures that resulted from jet-on staging caused high pressures upstream of the base on the second-stage afterbody. This effect is shown in figure 12. In nearly all cases the magnitude of the pressure rise approached that necessary to cause flow separation. These high pressures could cause undesirable second-stage moments if the distribution were not uniform circumferentially, as might occur during unstable flow and/or during stage misalinement. The extent of this pressure disturbance upstream of the base indicated by the position where local static pressures began to exceed ambient pressure is summarized in figure 13. Without ports (fig. 13(a)), increasing the diameter ratio from 1.25 to 1.5 caused the disturbance to move upstream; however, with ports (fig. 13(b)), this increase in diameter ratio decreased the extent of the disturbance. This decrease indicates that with ports the pressure disturbance on the second-stage afterbody was strongly influenced by the interaction of the port flow and the stream, since the ports were located farther aft with the diameter-ratio-1.5 configuration than with diameter ratio 1.25. As expected, the use of ports markedly reduced the extent of the disturbance.

Figure 14 presents selected schlieren photographs depicting the flow field that exists for the data points indicated in figure 11. From these can be seen the effects of higher-than-ambient base pressures (photographs 1 to 4 and 6 and 7), separation of flow on the second-stage afterbody with high base-region pressures moving onto the afterbody (photograph 6), and changes in rocket flow due to first-stage interference effects on the base as the first stage moves downstream (photographs 4, 5, 7, and 8).

SUMMARY OF RESULTS

Interstage aerodynamic pressures on a two-stage missile having a constant-total-pressure second-stage cold-air jet and a sting-mounted translating first stage were investigated for a range of separation distances at Mach 2 and a pressure altitude of 38,000 feet. The following results were obtained:

Jet-off:

1. First-stage interference effects produced second-stage base pressures higher than ambient pressure for separation distances to at least 2.8 second-stage diameters. Increasing stage diameter ratio increased base pressure for separation distances up to 1.8 diameters but had little effect thereafter.

2. Misalinement of stage centerlines resulted in unstable interstage flow. The magnitude of the misalinement necessary to cause this instability increases as separation distance increases.

Jet-on:

1. For separation distances up to about 2 second-stage diameters, the second-stage base pressures were considerably higher than jet-off base pressures, but at greater distances the interference effects of the first stage had disappeared. Ports in the first-stage forebody reduced the range of separation distance over which interference effects were felt.

2. Without first-stage ports, widely fluctuating interstage pressures were experienced for separation distances of about 1 second-stage diameter. The use of ports reduced but did not eliminate these effects.

3. The use of ports generally reduced the extent of second-stage afterbody pressure disturbances.

Lewis Research Center
National Aeronautics and Space Administration
Cleveland, Ohio, January 30, 1961

REFERENCES

1. Beheim, Milton A.: Flow in the Base Region of Axisymmetric and Two-Dimensional Configurations. NASA TR R-77, 1961.

2. Baughman, L. Eugene, and Kochendorfer, Fred D.: Jet Effects on Base Pressures of Conical Afterbodies at Mach 1.91 and 3.12. NACA RM E57E06, 1957.

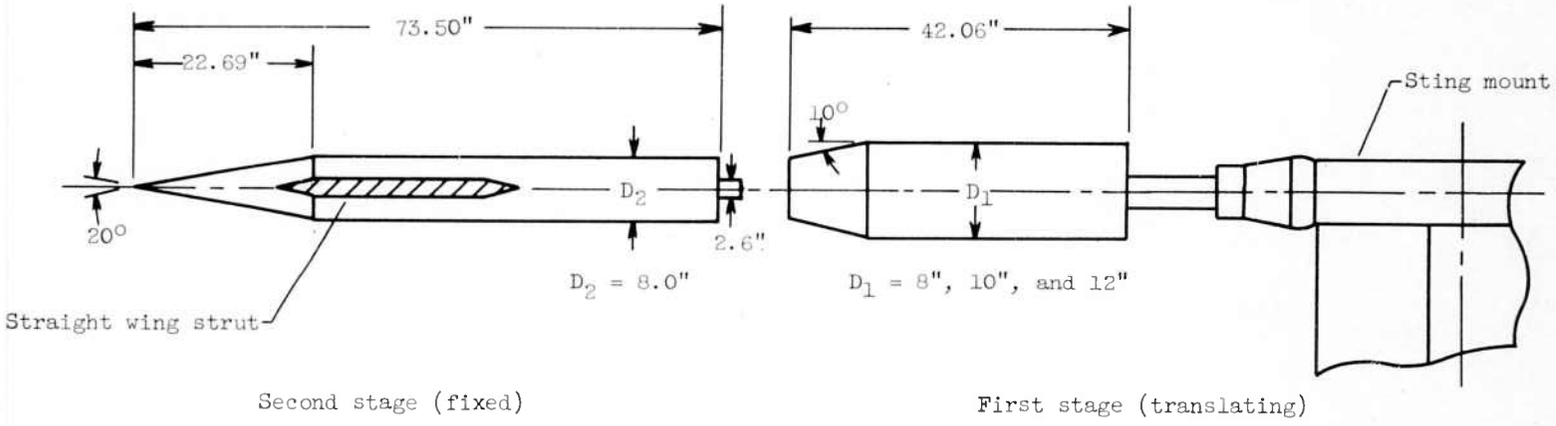

(a) Model schematic.

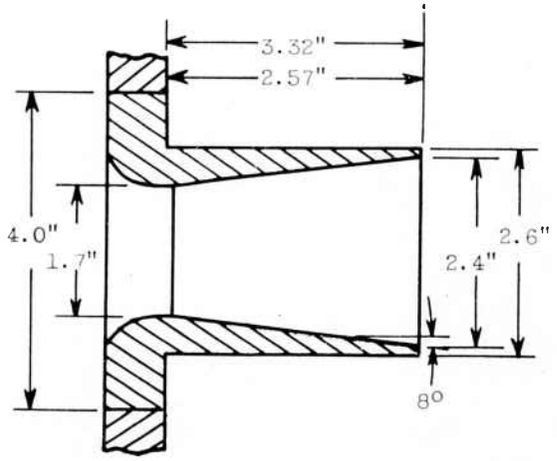

(b) Nozzle details.

Figure 1. - Model schematic and nozzle details.

Typical slot for 10"
and 12" first stage

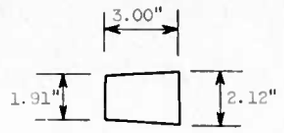

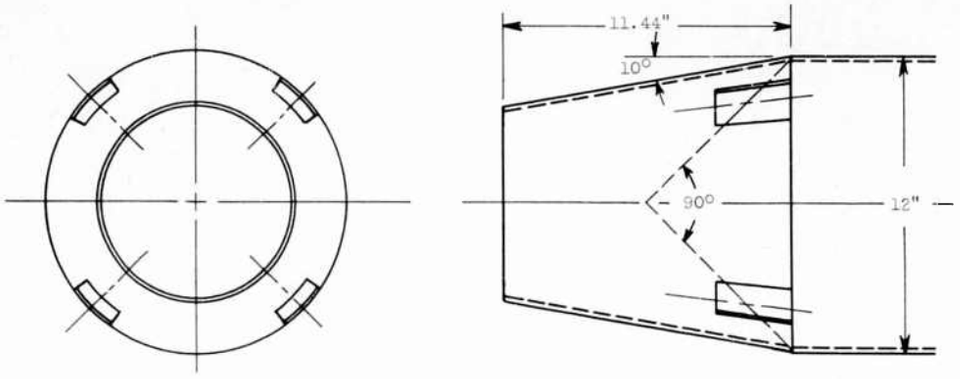

(a) Diameter ratio, D_1/D_2, 1.5.

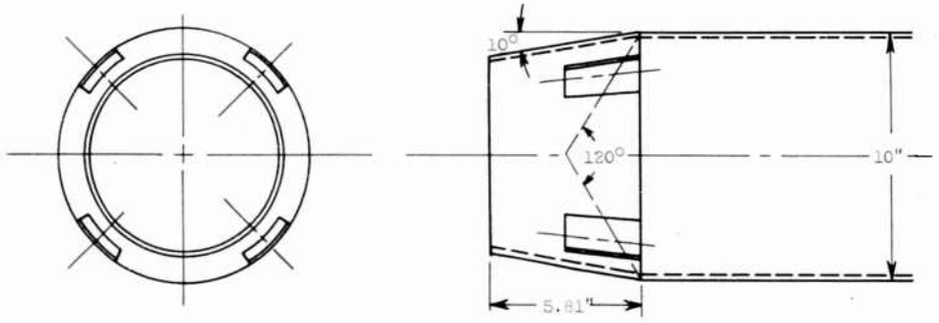

(b) Diameter ratio, D_1/D_2, 1.25.

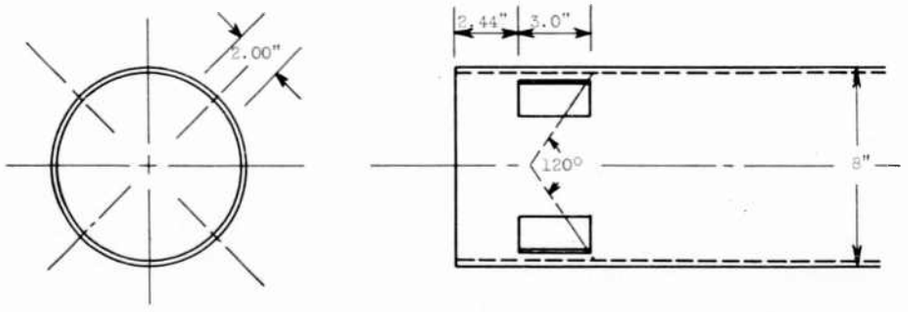

(c) Diameter ratio, D_1/D_2, 1.0.

Figure 2. - First-stage geometry including port and deflector details.

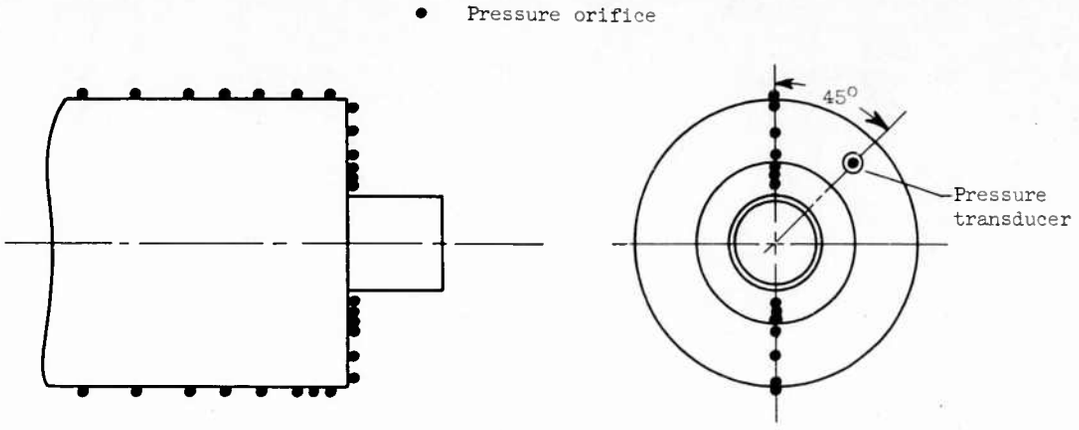

(a) Second stage.

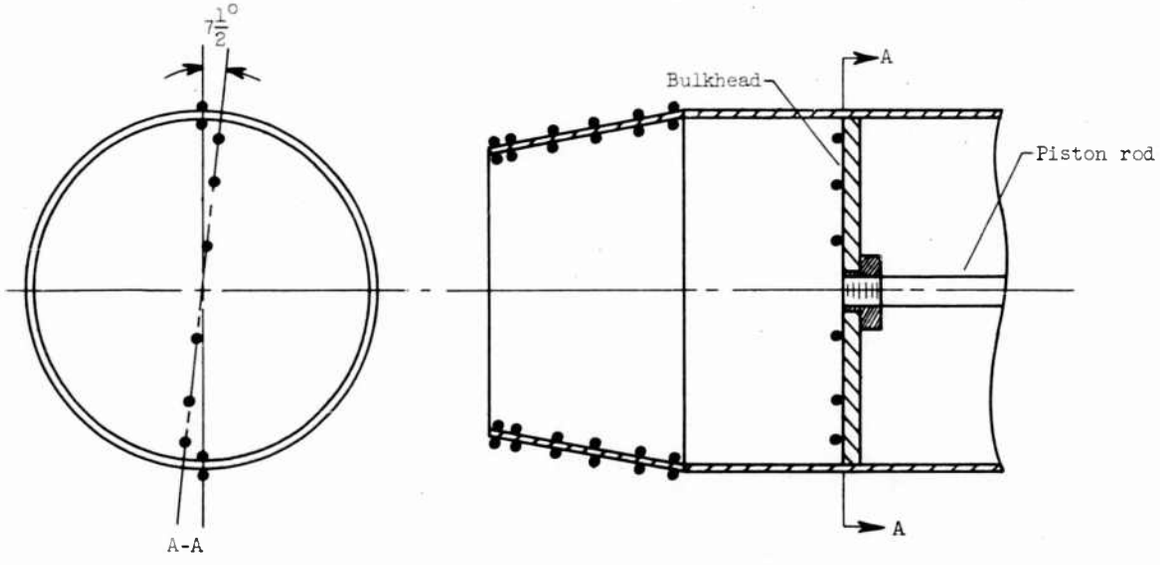

(b) First stage, no ports.

Figure 3. - Model instrumentation.

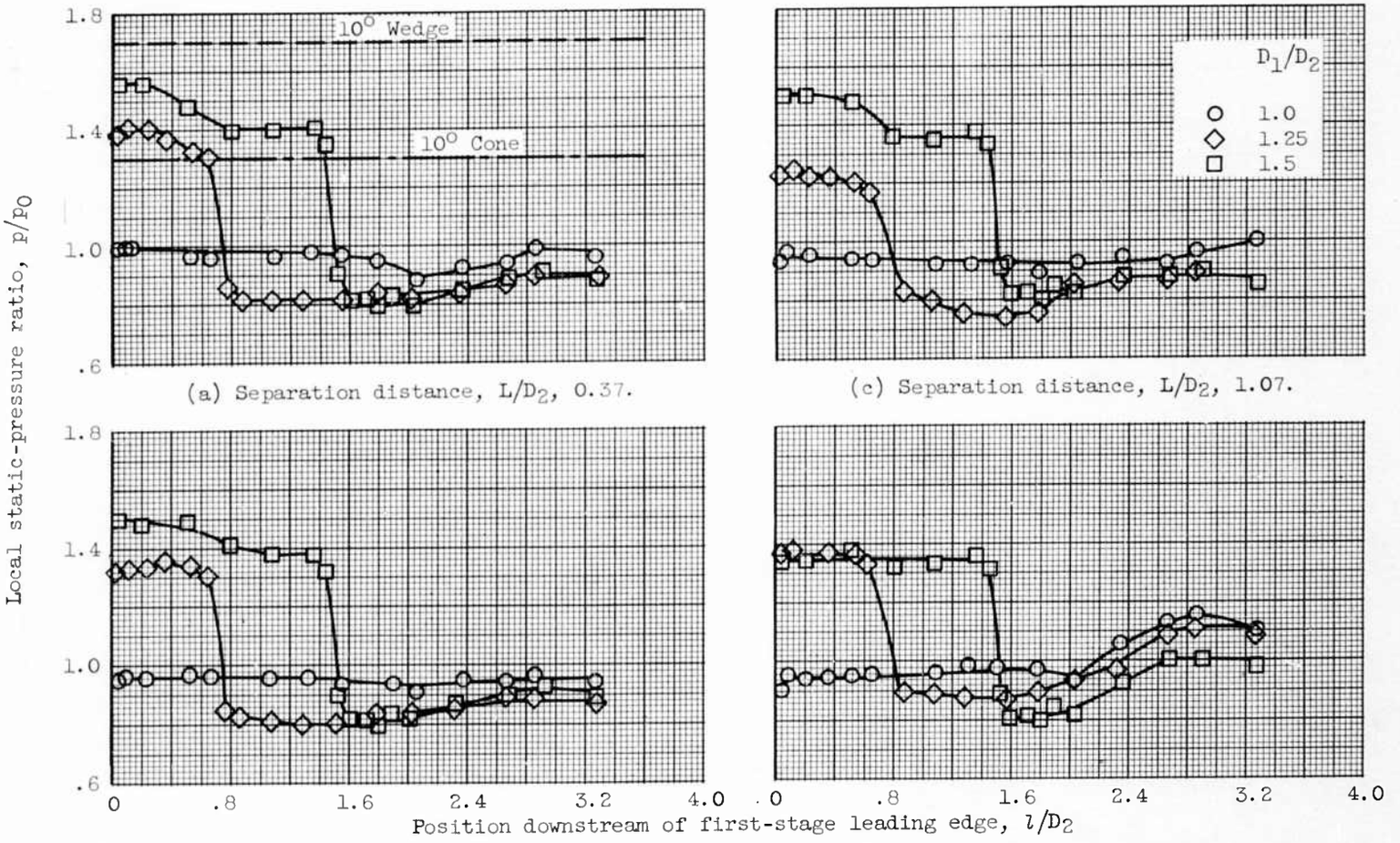

(a) Separation distance, L/D_2, 0.37.

(c) Separation distance, L/D_2, 1.07.

(b) Separation distance, L/D_2, 0.62.

(d) Separation distance, L/D_2, 2.12.

Figure 4. - First-stage external pressure distributions; jet-off.

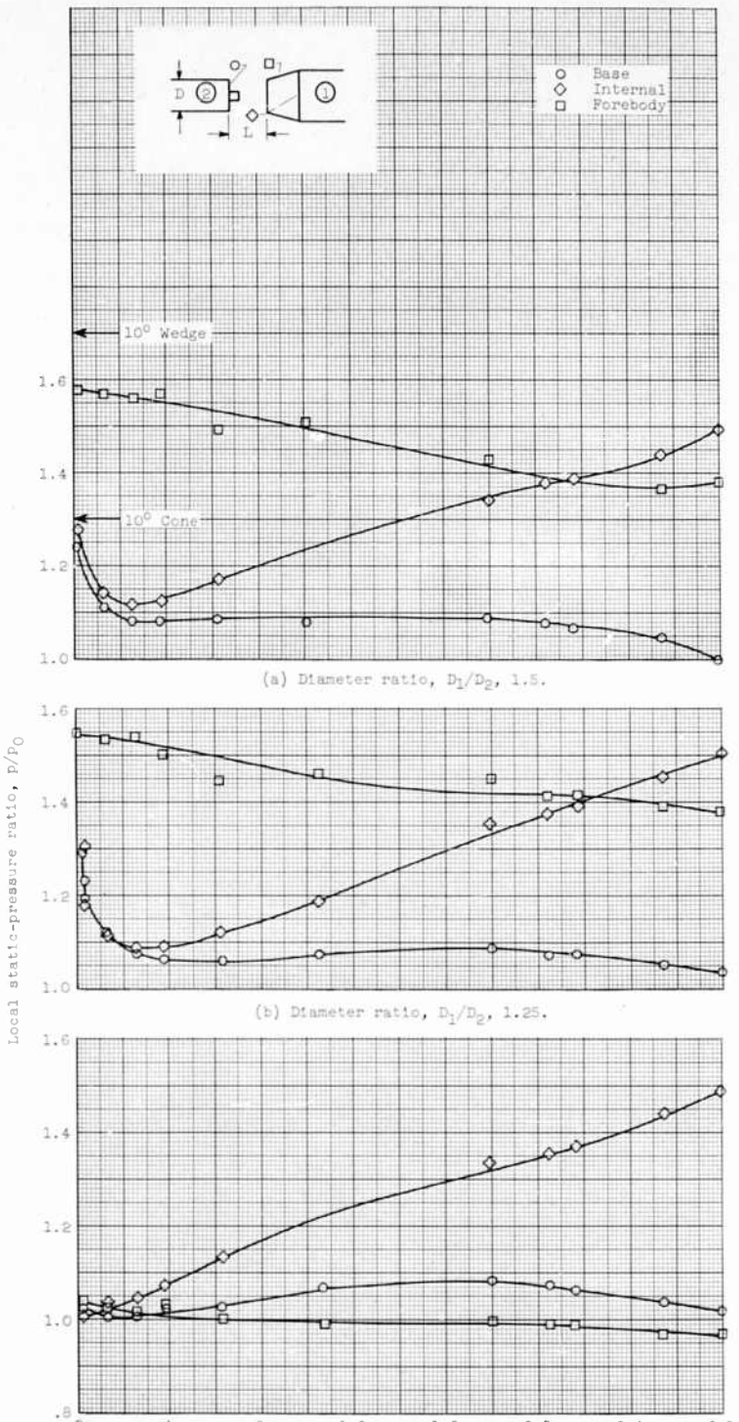

(a) Diameter ratio, D_1/D_2, 1.5.

(b) Diameter ratio, D_1/D_2, 1.25.

(c) Diameter ratio, D_1/D_2, 1.0.

Figure 5. - Effect of separation distance on first- and second-stage pressures; jet-off, no first-stage ports.

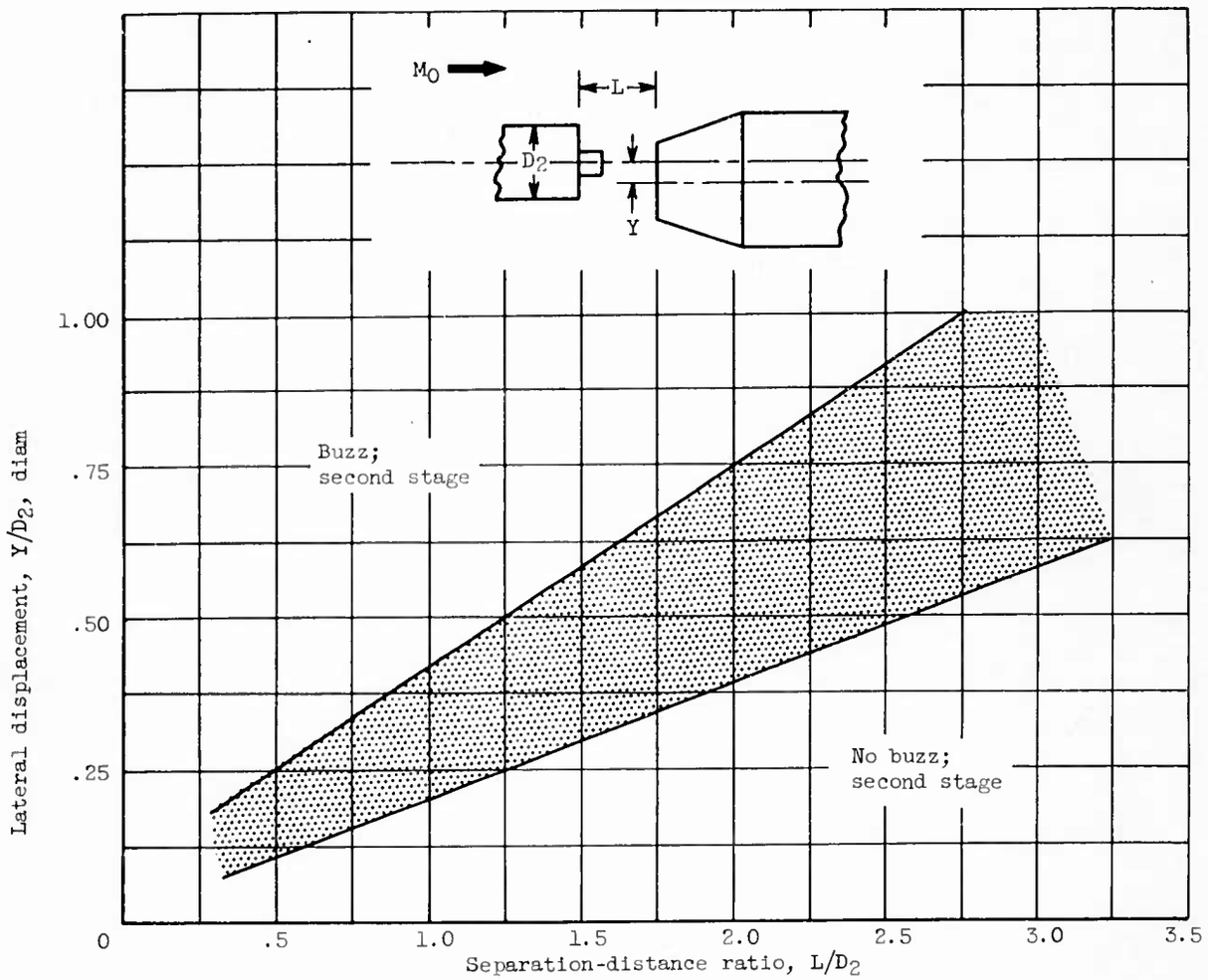

Figure 6. - Effect of separation distance and lateral displacement on pressure fluctuations at base of second stage; jet-off.

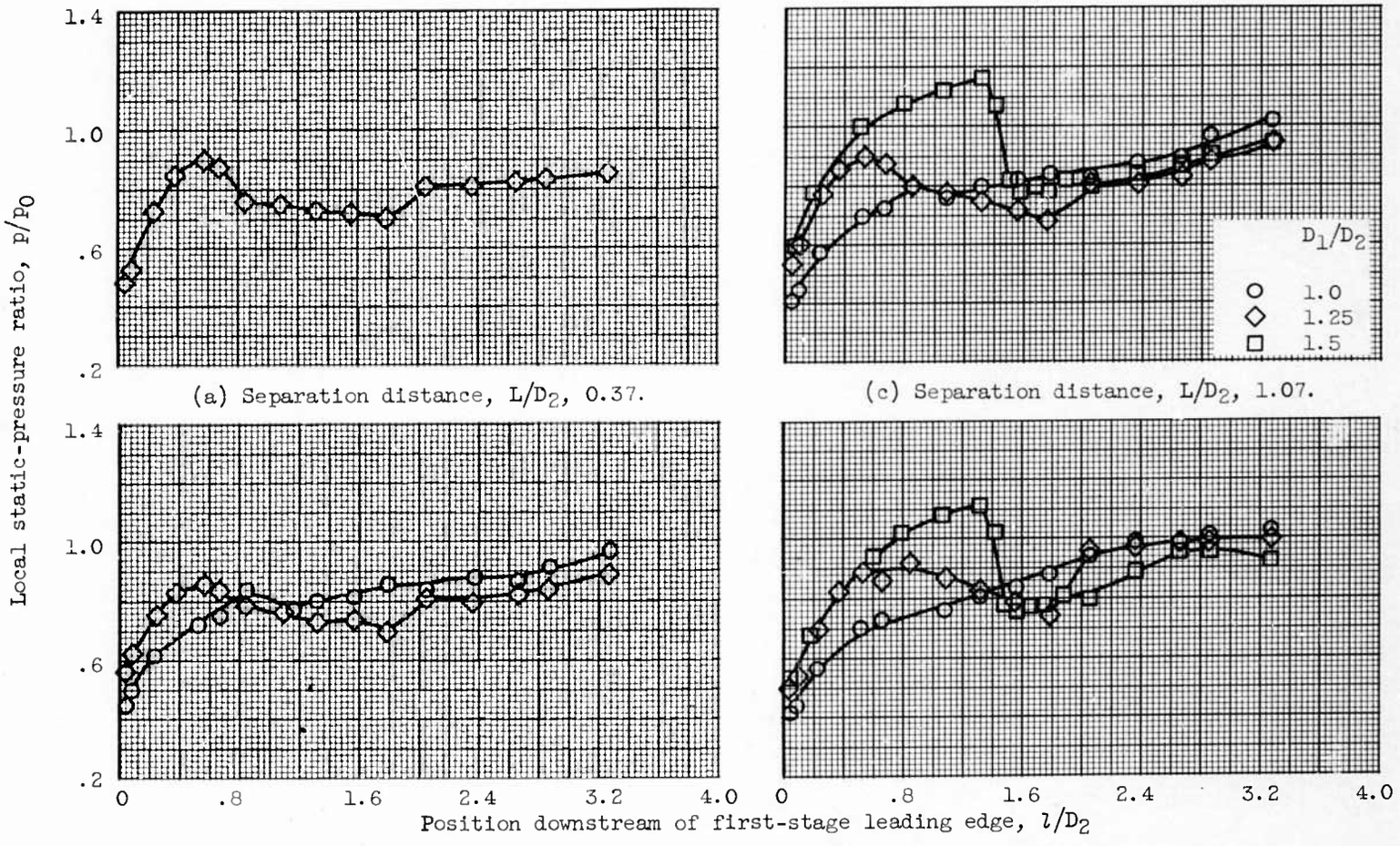

(a) Separation distance, L/D_2, 0.37.

(c) Separation distance, L/D_2, 1.07.

(b) Separation distance, L/D_2, 0.62.

(d) Separation distance, L/D_2, 2.12.

Figure 7. - First-stage external pressure distributions; jet-on; no ports.

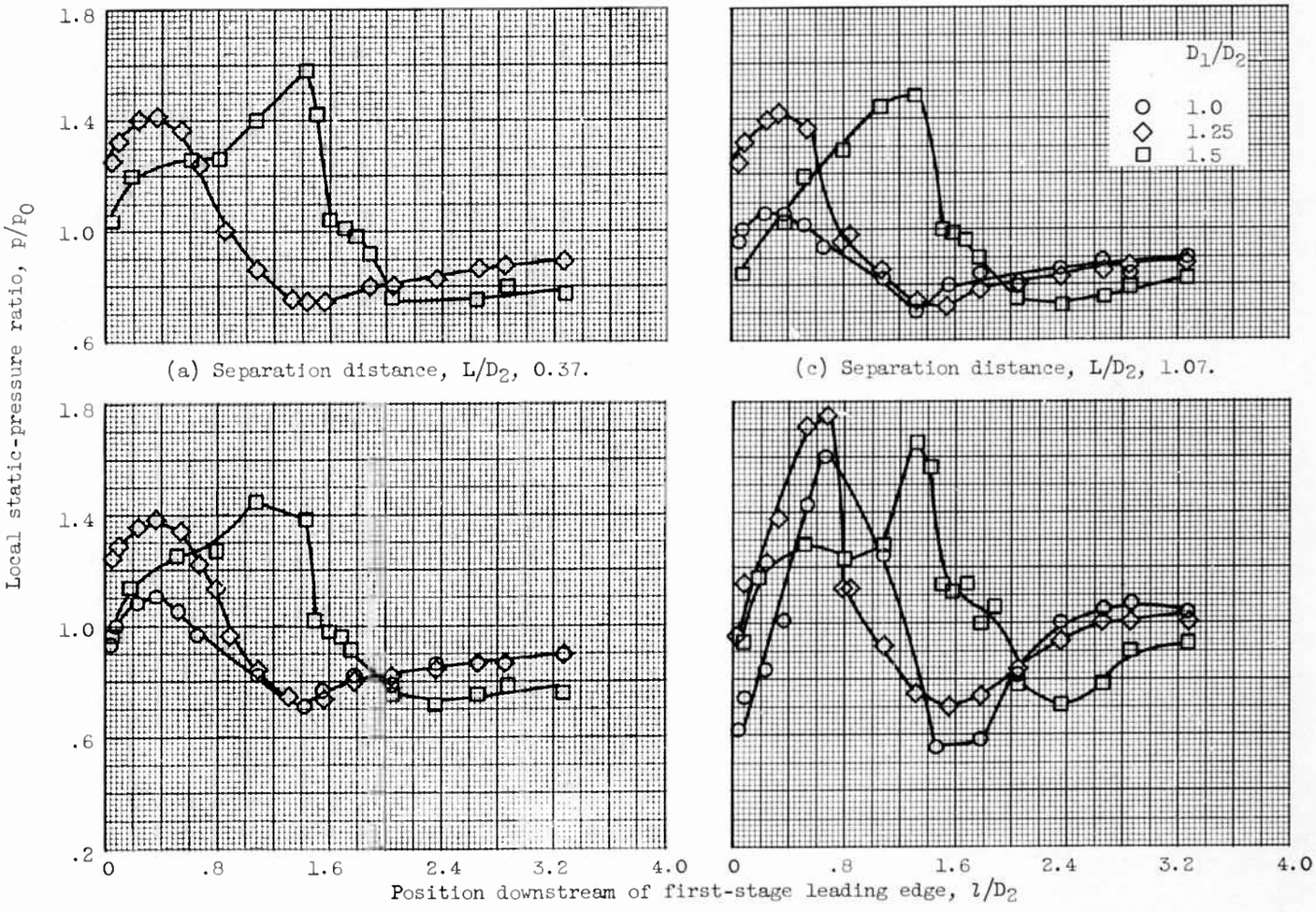

(a) Separation distance, L/D_2, 0.37.

(c) Separation distance, L/D_2, 1.07.

(b) Separation distance, L/D_2, 0.62.

(d) Separation distance, L/D_2, 2.12.

Figure 8. - First-stage external pressure distributions; jet-on; ports.

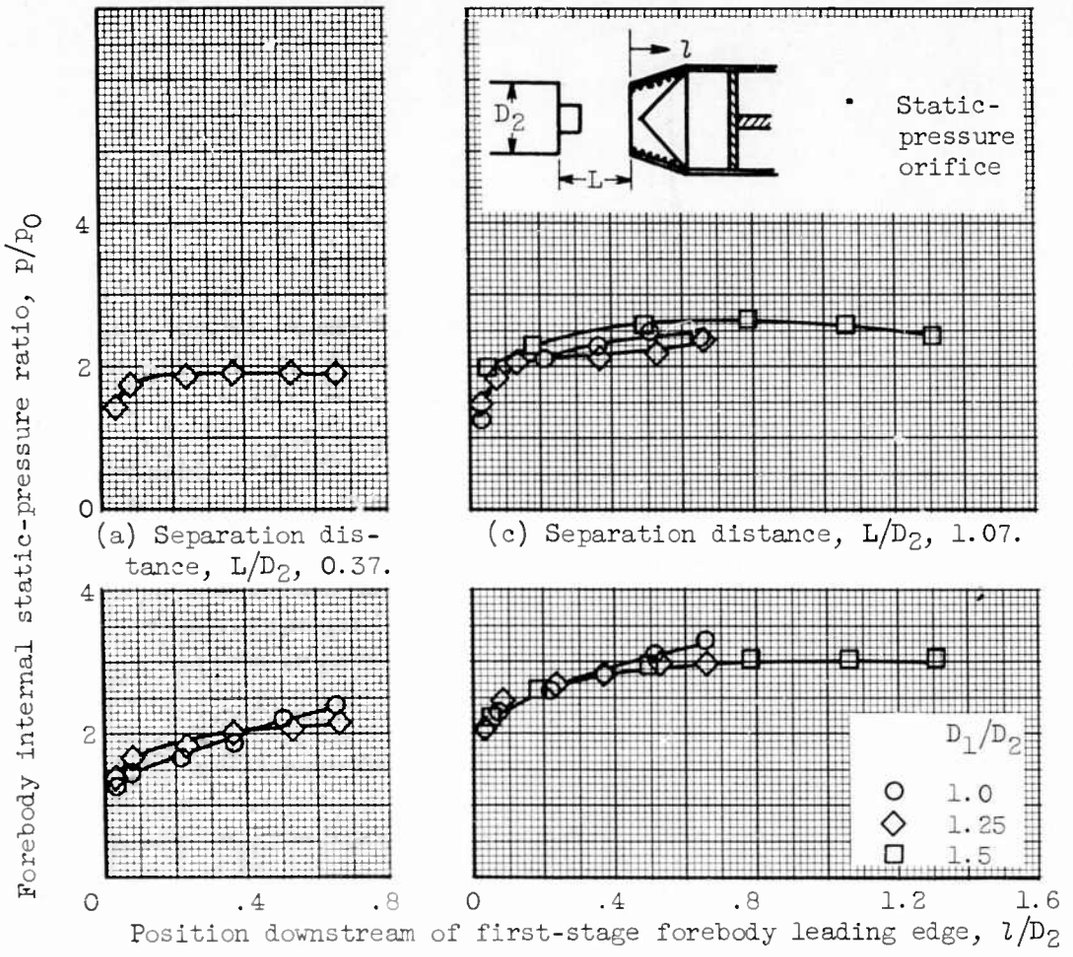

(a) Separation distance, L/D_2, 0.37.

(b) Separation distance, L/D_2, 0.62.

(c) Separation distance, L/D_2, 1.07.

(d) Separation distance, L/D_2, 2.12.

Figure 9. - First-stage forebody internal pressure distributions; jet-on; no ports.

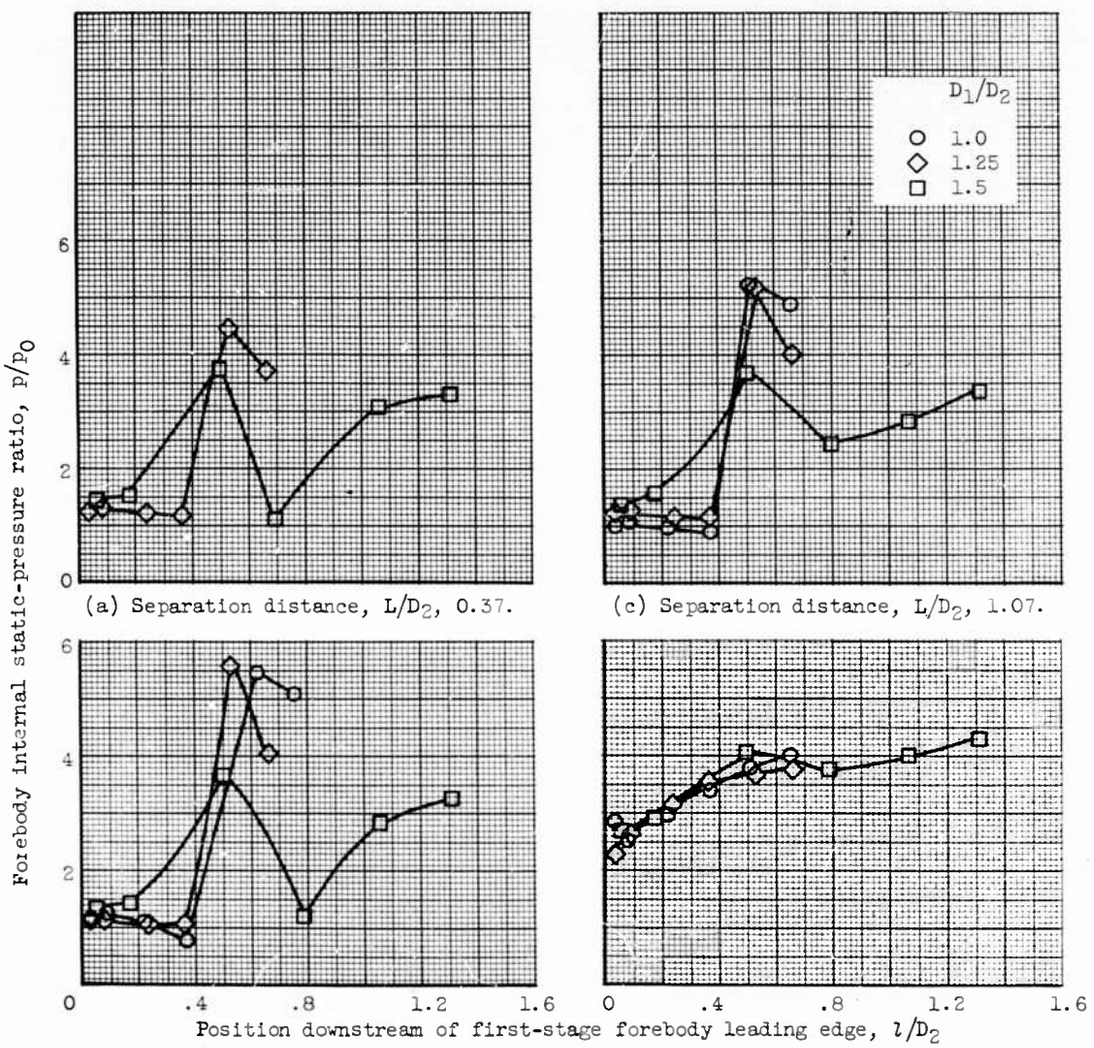

(a) Separation distance, L/D_2, 0.37.

(c) Separation distance, L/D_2, 1.07.

(b) Separation distance, L/D_2, 0.62.

(d) Separation distance, L/D_2, 2.12.

Figure 10. - First-stage forebody internal pressure distribution; jet-on; ports.

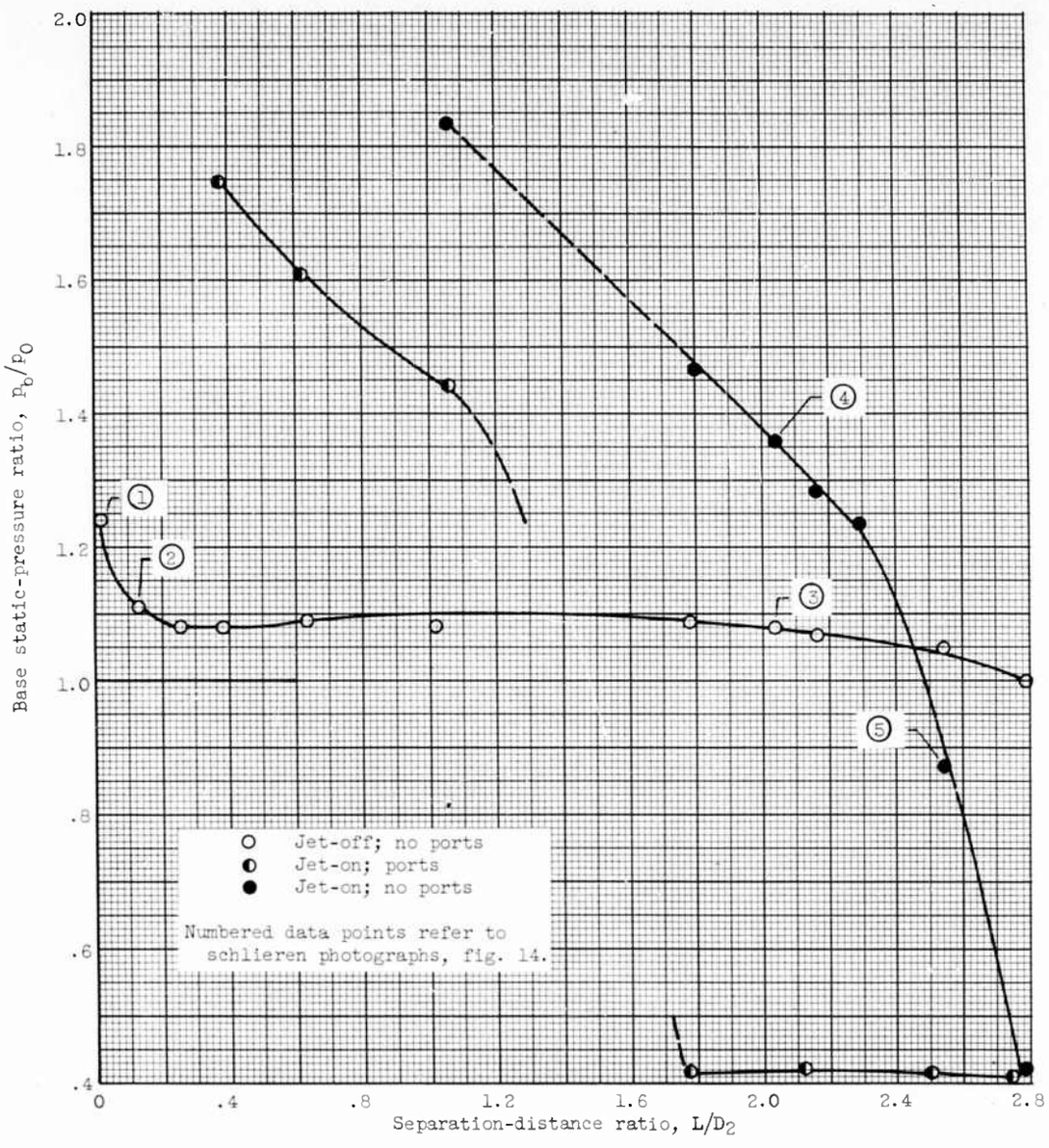

(a) Diameter ratio, D_1/D_2, 1.5.

Figure 11. - Effect of separation distance on second-stage base pressure.

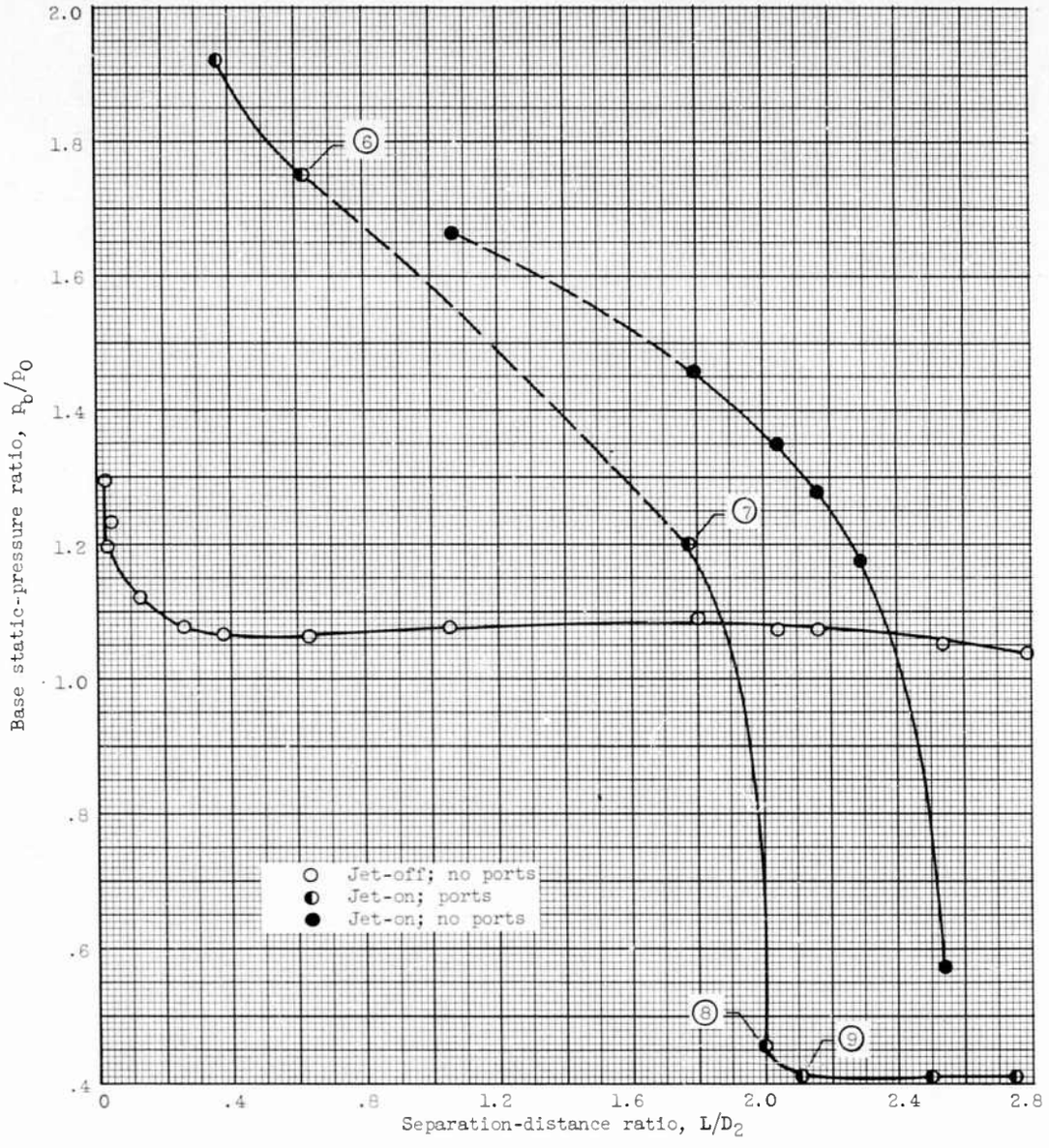

(b) Diameter ratio, D_1/D_2, 1.25.

Figure 11. - Continued. Effect of separation distance on second-stage base pressure.

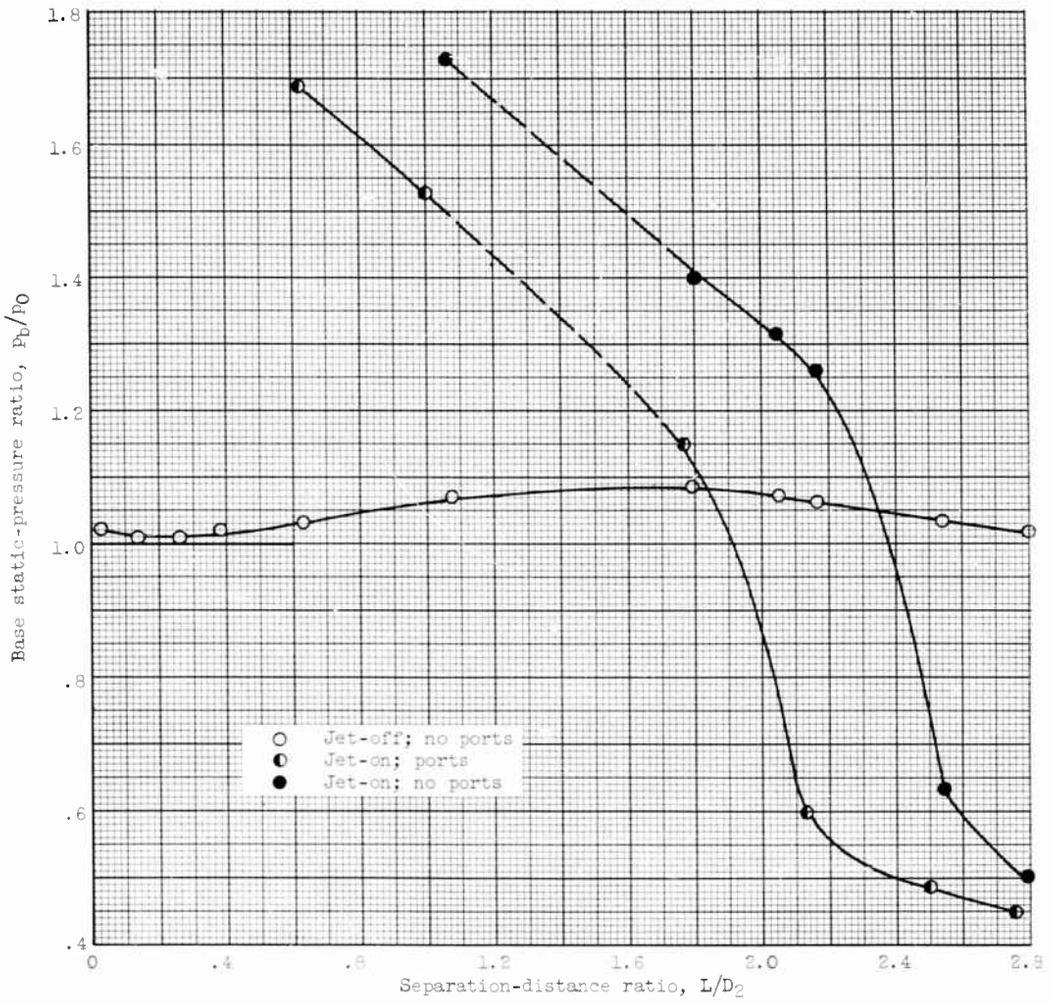

(c) Diameter ratio, D_1/D_2, 1.0.

Figure 11. - Concluded. Effect of separation distance on second-stage base pressure.

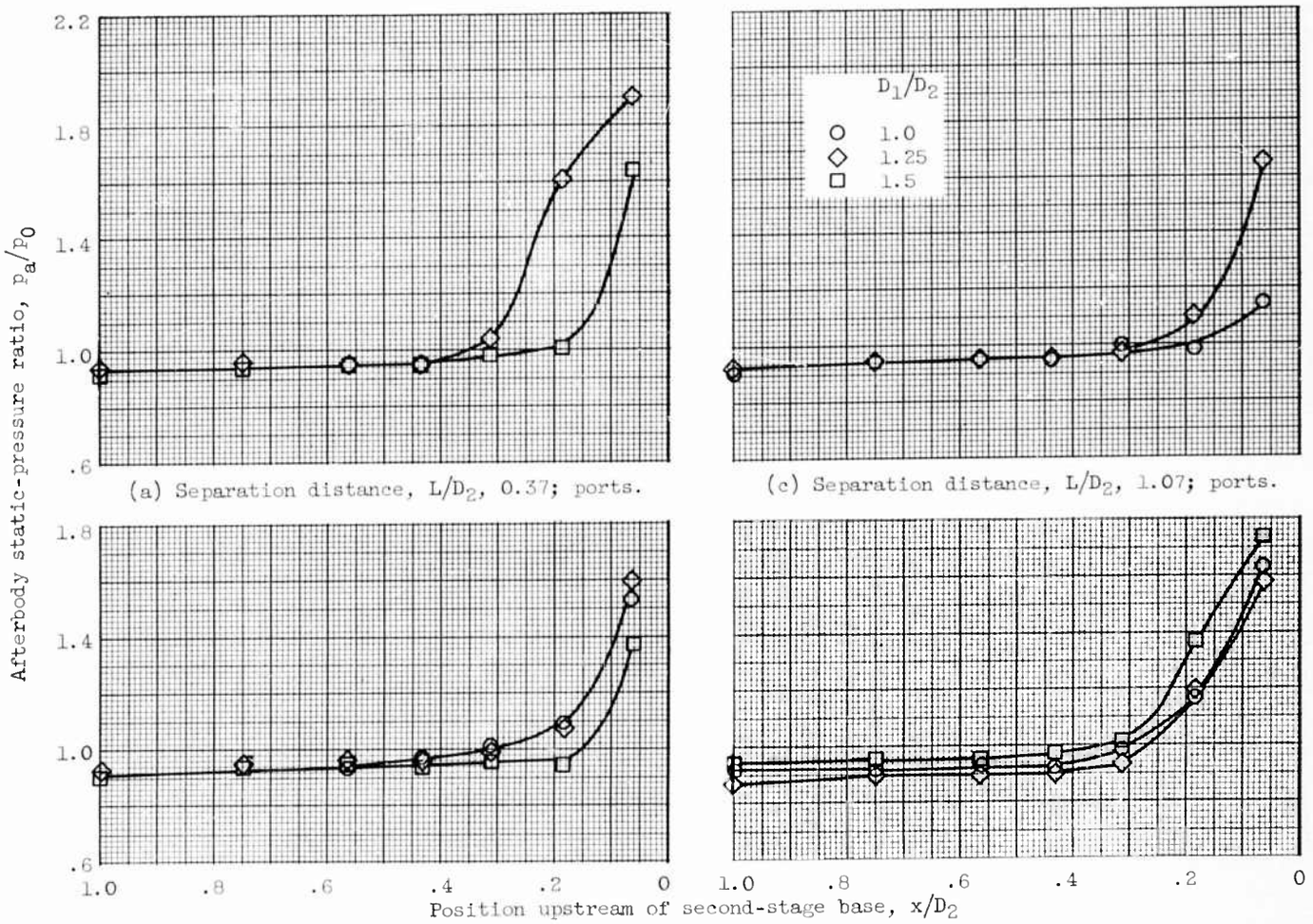

(a) Separation distance, L/D_2, 0.37; ports.

(c) Separation distance, L/D_2, 1.07; ports.

(b) Separation distance, L/D_2, 0.62; ports.

(d) Separation distance, L/D_2, 1.07; no ports.

Figure 12. - Second-stage afterbody pressure distributions; jet-on.

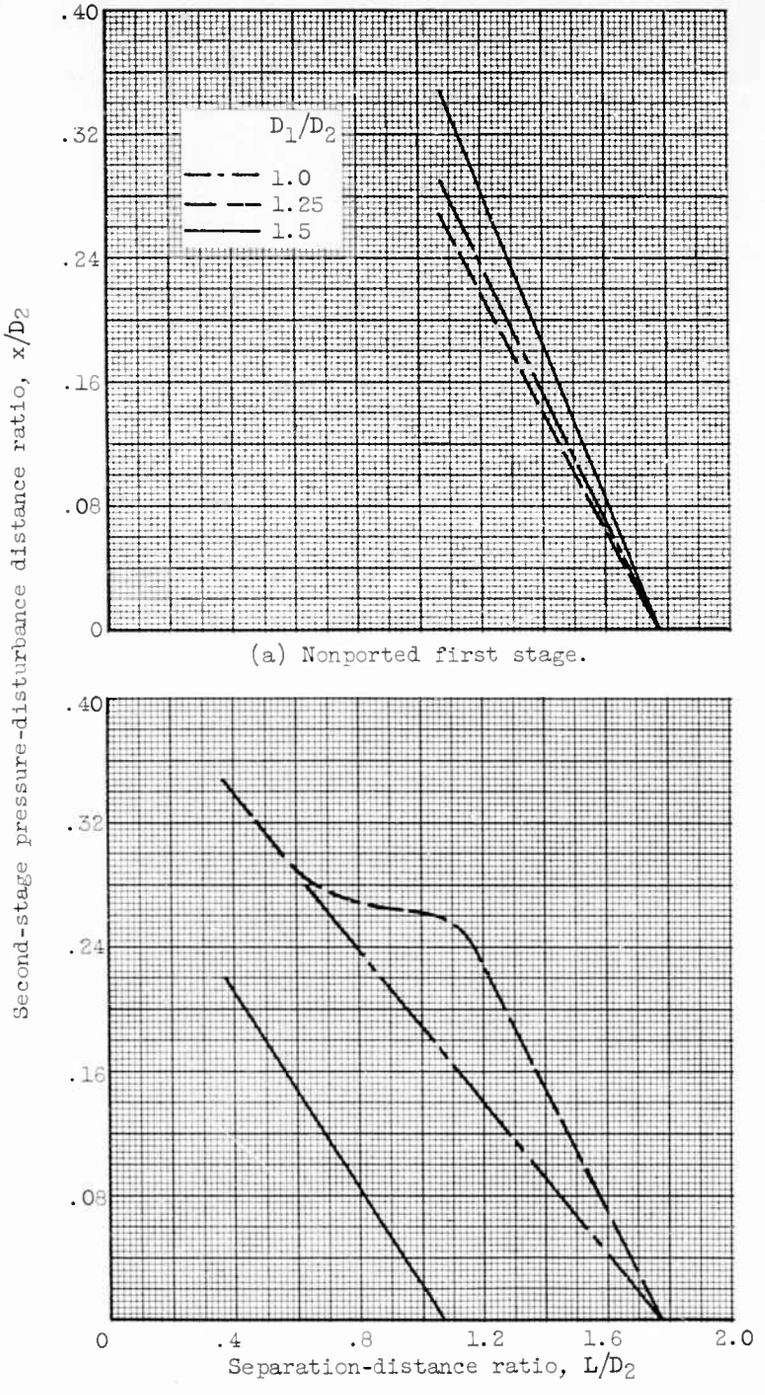

(a) Nonported first stage.

(b) Ported first stage.

Figure 13. - Effect of separation distance and ports on location of second-stage pressure disturbance.

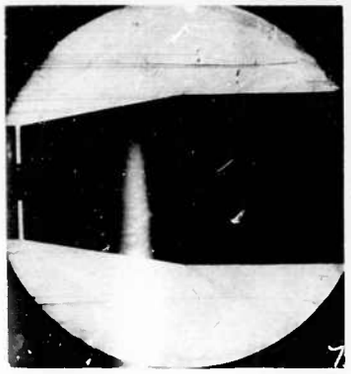

(1) D_1/D_2, 1.5; L/D_2, 0.013; p_b/p_0, 1.24.

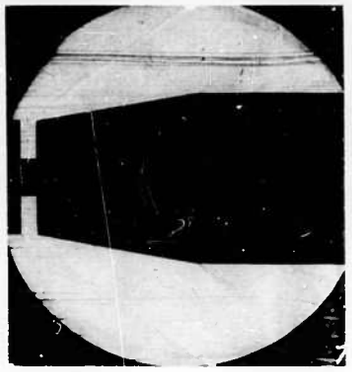

(2) D_1/D_2, 1.5; L/D_2, 0.125; p_b/p_0, 1.11.

(3) D_1/D_2, 1.5; L/D_2, 2.039; p_b/p_0, 1.074.

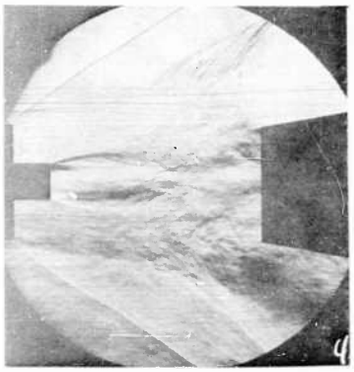

(4) D_1/D_2, 1.5; L/D_2, 2.039; p_b/p_0, 1.355.

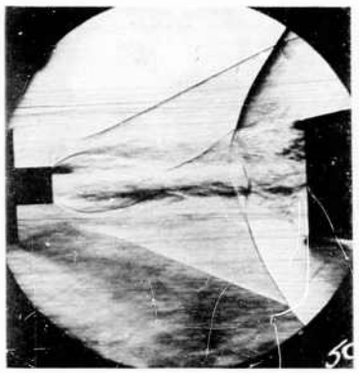

(5) D_1/D_2, 1.5; L/D_2, 2.539; p_b/p_0, 0.87.

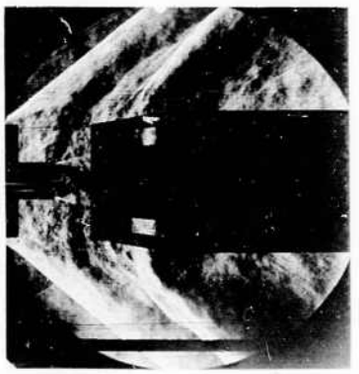

(6) D_1/D_2, 1.25; L/D_2, 0.625; p_b/p_0, 1.75.

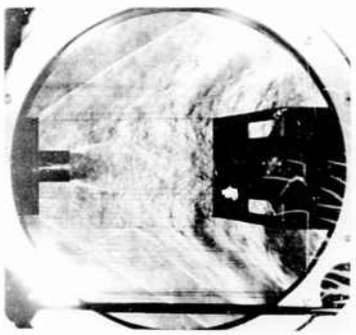

(7) D_1/D_2, 1.25; L/D_2, 1.789; p_b/p_0, 1.20.

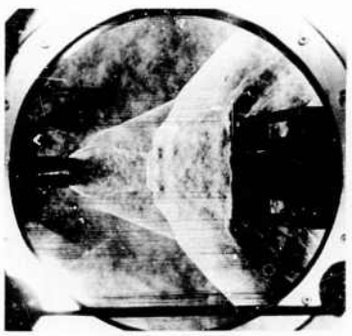

(8) D_1/D_2, 1.25; L/D_2, 2.039; p_b/p_0, 0.45.

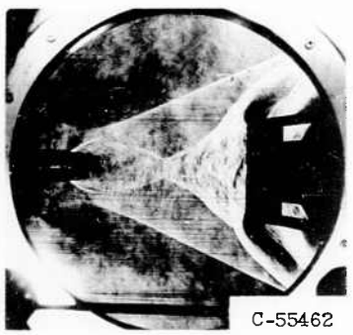

(9) D_1/D_2, 1.25; L/D_2, 2.164; p_b/p_0, 0.41.

Figure 14. - Schlieren photographs of model.

E-1103